



Measurement of the $B^0\text{-}\overline{B}^0$ Mixing Parameter Δm_d using Semileptonic B^0 Decays

K. Hara,³² M. Hazumi,⁹ K. Abe,⁹ K. Abe,⁴³ T. Abe,⁴⁴ I. Adachi,⁹ Byoung Sup Ahn,¹⁶
H. Aihara,⁴⁵ M. Akatsu,²³ Y. Asano,⁵⁰ T. Aso,⁴⁹ V. Aulchenko,² T. Aushev,¹³
A. M. Bakich,⁴⁰ Y. Ban,³⁴ A. Bay,¹⁹ I. Bedny,² P. K. Behera,⁵¹ I. Bizjak,¹⁴ A. Bondar,²
A. Bozek,²⁸ M. Bračko,^{21,14} J. Brodzicka,²⁸ T. E. Browder,⁸ B. C. K. Casey,⁸
P. Chang,²⁷ Y. Chao,²⁷ K.-F. Chen,²⁷ B. G. Cheon,³⁹ R. Chistov,¹³ S.-K. Choi,⁷
Y. Choi,³⁹ Y. K. Choi,³⁹ M. Danilov,¹³ L. Y. Dong,¹¹ J. Dragic,²² S. Eidelman,²
V. Eiges,¹³ Y. Enari,²³ C. W. Everton,²² F. Fang,⁸ C. Fukunaga,⁴⁷ N. Gabyshev,⁹
A. Garmash,^{2,9} T. Gershon,⁹ B. Golob,^{20,14} R. Guo,²⁵ J. Haba,⁹ K. Hanagaki,³⁵
F. Handa,⁴⁴ T. Hara,³² N. C. Hastings,²² H. Hayashii,²⁴ E. M. Heenan,²² I. Higuchi,⁴⁴
T. Higuchi,⁴⁵ L. Hinz,¹⁹ Y. Hoshi,⁴³ W.-S. Hou,²⁷ Y. B. Hsiung,^{27,*} S.-C. Hsu,²⁷
H.-C. Huang,²⁷ T. Igaki,²³ Y. Igarashi,⁹ T. Iijima,²³ K. Inami,²³ A. Ishikawa,²³ R. Itoh,⁹
H. Iwasaki,⁹ Y. Iwasaki,⁹ H. K. Jang,³⁸ H. Kakuno,⁴⁶ J. H. Kang,⁵⁴ J. S. Kang,¹⁶
N. Katayama,⁹ H. Kawai,³ Y. Kawakami,²³ N. Kawamura,¹ H. Kichimi,⁹ D. W. Kim,³⁹
Heejong Kim,⁵⁴ H. J. Kim,⁵⁴ Hyunwoo Kim,¹⁶ T. H. Kim,⁵⁴ K. Kinoshita,⁵ S. Korpar,^{21,14}
P. Križan,^{20,14} P. Krokovny,² R. Kulasiri,⁵ S. Kumar,³³ A. Kuzmin,² Y.-J. Kwon,⁵⁴
J. S. Lange,^{6,36} G. Leder,¹² S. H. Lee,³⁸ J. Li,³⁷ R.-S. Lu,²⁷ J. MacNaughton,¹²
G. Majumder,⁴¹ F. Mandl,¹² T. Matsuishi,²³ S. Matsumoto,⁴ T. Matsumoto,⁴⁷
K. Miyabayashi,²⁴ Y. Miyabayashi,²³ H. Miyata,³⁰ G. R. Moloney,²² T. Mori,⁴
T. Nagamine,⁴⁴ Y. Nagasaka,¹⁰ T. Nakadaira,⁴⁵ E. Nakano,³¹ M. Nakao,⁹ J. W. Nam,³⁹
Z. Natkaniec,²⁸ S. Nishida,¹⁷ O. Nitoh,⁴⁸ S. Noguchi,²⁴ T. Nozaki,⁹ S. Ogawa,⁴²
T. Ohshima,²³ T. Okabe,²³ S. Okuno,¹⁵ S. L. Olsen,⁸ Y. Onuki,³⁰ W. Ostrowicz,²⁸
H. Ozaki,⁹ H. Palka,²⁸ C. W. Park,¹⁶ H. Park,¹⁸ L. S. Peak,⁴⁰ J.-P. Perroud,¹⁹
M. Peters,⁸ L. E. Piilonen,⁵² N. Root,² M. Rozanska,²⁸ K. Rybicki,²⁸ H. Sagawa,⁹
S. Saitoh,⁹ Y. Sakai,⁹ H. Sakamoto,¹⁷ M. Satapathy,⁵¹ A. Satpathy,^{9,5} O. Schneider,¹⁹
S. Schrenk,⁵ C. Schwanda,^{9,12} S. Semenov,¹³ K. Senyo,²³ R. Seuster,⁸ M. E. Sevier,²²
H. Shibuya,⁴² B. Shwartz,² J. B. Singh,³³ N. Soni,³³ S. Stanič,^{50,†} M. Starič,¹⁴ A. Sugi,²³
A. Sugiyama,²³ K. Sumisawa,⁹ T. Sumiyoshi,⁴⁷ S. Suzuki,⁵³ S. Y. Suzuki,⁹ T. Takahashi,³¹
F. Takasaki,⁹ N. Tamura,³⁰ J. Tanaka,⁴⁵ M. Tanaka,⁹ G. N. Taylor,²² Y. Teramoto,³¹
S. Tokuda,²³ M. Tomoto,⁹ T. Tomura,⁴⁵ K. Trabelsi,⁸ T. Tsuboyama,⁹ T. Tsukamoto,⁹
S. Uehara,⁹ K. Ueno,²⁷ Y. Unno,³ S. Uno,⁹ Y. Ushiroda,⁹ G. Varner,⁸ K. E. Varvell,⁴⁰
C. C. Wang,²⁷ C. H. Wang,²⁶ J. G. Wang,⁵² M.-Z. Wang,²⁷ Y. Watanabe,⁴⁶ E. Won,¹⁶
B. D. Yabsley,⁵² Y. Yamada,⁹ A. Yamaguchi,⁴⁴ Y. Yamashita,²⁹ M. Yamauchi,⁹ H. Yanai,³⁰
M. Yokoyama,⁴⁵ Y. Yuan,¹¹ Y. Yusa,⁴⁴ Z. P. Zhang,³⁷ V. Zhilich,² and D. Žontar⁵⁰

(The Belle Collaboration)

¹*Aomori University, Aomori*

²*Budker Institute of Nuclear Physics, Novosibirsk*

- ³*Chiba University, Chiba*
⁴*Chuo University, Tokyo*
⁵*University of Cincinnati, Cincinnati OH*
⁶*University of Frankfurt, Frankfurt*
⁷*Gyeongsang National University, Chinju*
⁸*University of Hawaii, Honolulu HI*
⁹*High Energy Accelerator Research Organization (KEK), Tsukuba*
¹⁰*Hiroshima Institute of Technology, Hiroshima*
¹¹*Institute of High Energy Physics,
Chinese Academy of Sciences, Beijing*
¹²*Institute of High Energy Physics, Vienna*
¹³*Institute for Theoretical and Experimental Physics, Moscow*
¹⁴*J. Stefan Institute, Ljubljana*
¹⁵*Kanagawa University, Yokohama*
¹⁶*Korea University, Seoul*
¹⁷*Kyoto University, Kyoto*
¹⁸*Kyungpook National University, Taegu*
¹⁹*Institut de Physique des Hautes Énergies, Université de Lausanne, Lausanne*
²⁰*University of Ljubljana, Ljubljana*
²¹*University of Maribor, Maribor*
²²*University of Melbourne, Victoria*
²³*Nagoya University, Nagoya*
²⁴*Nara Women's University, Nara*
²⁵*National Kaohsiung Normal University, Kaohsiung*
²⁶*National Lien-Ho Institute of Technology, Miao Li*
²⁷*National Taiwan University, Taipei*
²⁸*H. Niewodniczanski Institute of Nuclear Physics, Krakow*
²⁹*Nihon Dental College, Niigata*
³⁰*Niigata University, Niigata*
³¹*Osaka City University, Osaka*
³²*Osaka University, Osaka*
³³*Panjab University, Chandigarh*
³⁴*Peking University, Beijing*
³⁵*Princeton University, Princeton NJ*
³⁶*RIKEN BNL Research Center, Brookhaven NY*
³⁷*University of Science and Technology of China, Hefei*
³⁸*Seoul National University, Seoul*
³⁹*Sungkyunkwan University, Suwon*
⁴⁰*University of Sydney, Sydney NSW*
⁴¹*Tata Institute of Fundamental Research, Bombay*
⁴²*Toho University, Funabashi*
⁴³*Tohoku Gakuin University, Tagajo*
⁴⁴*Tohoku University, Sendai*
⁴⁵*University of Tokyo, Tokyo*
⁴⁶*Tokyo Institute of Technology, Tokyo*
⁴⁷*Tokyo Metropolitan University, Tokyo*
⁴⁸*Tokyo University of Agriculture and Technology, Tokyo*

⁴⁹*Toyama National College of Maritime Technology, Toyama*

⁵⁰*University of Tsukuba, Tsukuba*

⁵¹*Utkal University, Bhubaneswer*

⁵²*Virginia Polytechnic Institute and State University, Blacksburg VA*

⁵³*Yokkaichi University, Yokkaichi*

⁵⁴*Yonsei University, Seoul*

(Dated: May 17, 2019)

Abstract

We present a measurement of the B^0 - \bar{B}^0 mixing parameter Δm_d using neutral B meson pairs in a 29.1 fb^{-1} data sample collected at the $\Upsilon(4S)$ resonance with the Belle detector at the KEKB asymmetric-energy e^+e^- collider. We exclusively reconstruct one neutral B meson in the semileptonic $B^0 \rightarrow D^{*-}\ell^+\nu$ decay mode and identify the flavor of the accompanying B meson from its decay products. From the distribution of the time intervals between the two flavor-tagged B meson decay points, we obtain $\Delta m_d = (0.494 \pm 0.012 \pm 0.015) \text{ ps}^{-1}$, where the first error is statistical and the second error is systematic.

PACS numbers: PACS numbers: 11.30.Er, 12.15.Hh, 13.25.Hw

$B^0\text{-}\overline{B}^0$ mixing plays a unique role in the determination of basic parameters in the Standard Model (SM) of elementary particles. It is characterized by the oscillation frequency Δm_d , which is the difference between the two mass eigenvalues of neutral B meson states. In the SM, the mixing is due to second-order weak interactions known as box diagrams whose amplitudes involve V_{td} , an element of the quark mixing matrix [1]. The mixing also induces large time-dependent CP violation in neutral B meson decays, which has been observed recently [2, 3]. For such CP violation measurements, precise Δm_d measurements are important.

In this Letter, we report a Δm_d measurement with $B^0\overline{B}^0$ pairs produced at the $\Upsilon(4S)$ resonance. The time evolution is described as $e^{-|\Delta t|/\tau_{B^0}}/(4\tau_{B^0})\{1 \pm \cos(\Delta m_d \Delta t)\}$, where the plus (minus) sign is taken when the flavor of one B meson is opposite to (the same as) the other, τ_{B^0} is the lifetime of the neutral B meson and Δt is the proper time difference between the two B meson decays. We reconstruct one neutral B meson in semileptonic $B^0 \rightarrow D^{*-}\ell^+\nu$ decays [4]. The large branching fractions and distinctive final states of the semileptonic decay allow for the efficient isolation of a high-purity sample of B^0 decays. The accompanying B meson is not fully reconstructed; we determine its flavor from the properties of the decay products.

This measurement is based on a 29.1 fb^{-1} data sample, which contains 31.3 million $B\overline{B}$ pairs, collected with the Belle detector at the KEKB asymmetric-energy e^+e^- (3.5 on 8 GeV) collider [5] operating at the $\Upsilon(4S)$ resonance. At KEKB, the $\Upsilon(4S)$ is produced with a Lorentz boost of $\beta\gamma = 0.425$ nearly along the electron beamline (z). Since the B mesons are approximately at rest in the $\Upsilon(4S)$ center-of-mass system (cms), Δt can be determined from the displacement in z between the two B decay vertices: $\Delta t \simeq (z_{\text{rec}} - z_{\text{tag}})/\beta\gamma c \equiv \Delta z/\beta\gamma c$.

The Belle detector [6] is a large-solid-angle spectrometer that consists of a silicon vertex detector (SVD), a central drift chamber (CDC), an array of aerogel threshold Čerenkov counters (ACC), time-of-flight scintillation counters (TOF), and an electromagnetic calorimeter comprised of CsI(Tl) crystals (ECL) located inside a superconducting solenoid coil that provides a 1.5 T magnetic field. An iron flux-return located outside of the coil is instrumented to detect K_L^0 mesons and to identify muons (KLM).

We use the decay chain $B^0 \rightarrow D^{*-}\ell^+\nu$, $D^{*-} \rightarrow \overline{D}^0\pi^-$, and $\overline{D}^0 \rightarrow K^+\pi^-$, $K^+\pi^-\pi^0$ or $K^+\pi^-\pi^+\pi^-$. We require associated SVD hits and radial impact parameters $|dr| < 0.2\text{ cm}$ for all tracks. Track momenta in the laboratory frame for $\overline{D}^0 \rightarrow K^+\pi^-\pi^0$ decays are required to be larger than $0.2\text{ GeV}/c$, while no additional requirements are applied for the other modes. Charged kaons are identified by combining information from the TOF, ACC and dE/dx measurements in the CDC. For $\pi^0 \rightarrow \gamma\gamma$ candidates, we use pairs of photons with energies greater than 0.08 GeV that have an invariant mass within $0.011\text{ GeV}/c^2$ of m_{π^0} and a total momentum greater than $0.2\text{ GeV}/c$. For $\overline{D}^0 \rightarrow K^+\pi^-$ and $K^+\pi^-\pi^+\pi^-$ candidates, we use daughter combinations that are within $0.013\text{ GeV}/c^2$ of m_{D^0} ; for $\overline{D}^0 \rightarrow K^+\pi^-\pi^0$ we expand the mass window to -0.037 and $+0.023\text{ GeV}/c^2$. For $D^{*-} \rightarrow \overline{D}^0\pi^-$ decays, we combine \overline{D}^0 candidates with a low-momentum π^- (slow pion) that is reconstructed using a vertex constraint and require the mass difference between the D^{*-} and \overline{D}^0 candidates to be within $1\text{ MeV}/c^2$ of the nominal value. We reject D^{*-} candidates with cms momentum greater than $2.6\text{ GeV}/c$, which is beyond the kinematic limit for B meson decays.

For the associated lepton, we use electrons or muons that have an opposite charge to the D^{*-} candidate. Electron identification is based on a combination of CDC dE/dx information, the ACC response, and energy deposit of the associated ECL shower. Muons are identified by comparing information from the KLM to extrapolated charged parti-

cle trajectories. We require $1.4 < p_\ell^{\text{cms}} < 2.4$ GeV/ c , where p_ℓ^{cms} is the cms momentum of the lepton. The cms angle of the lepton with respect to the direction of the D^{*-} candidate is also required to be greater than 90 degrees. For $B^0 \rightarrow D^{*-}\ell^+\nu$ decays, the energies and momenta of the B meson and the $D^*\ell$ system in the cms satisfy $M_\nu^2 = (E_B^{\text{cms}} - E_{D^*\ell}^{\text{cms}})^2 - |\vec{p}_B^{\text{cms}}|^2 - |\vec{p}_{D^*\ell}^{\text{cms}}|^2 + 2|\vec{p}_B^{\text{cms}}||\vec{p}_{D^*\ell}^{\text{cms}}|\cos\theta_{B,D^*\ell}$, where M_ν is the neutrino mass and $\theta_{B,D^*\ell}$ is the angle between \vec{p}_B^{cms} and $\vec{p}_{D^*\ell}^{\text{cms}}$. We calculate $\cos\theta_{B,D^*\ell}$ setting $M_\nu = 0$. Figure 1 shows the $\cos\theta_{B,D^*\ell}$ distribution. The signal region is defined as $|\cos\theta_{B,D^*\ell}| < 1.1$. We also require the candidate $D^{*-}\ell^+\nu$ decays to be outside the signal region when we artificially reverse the lepton momentum vector; this reduces an uncertainty in the estimation of the background fraction, as described below.

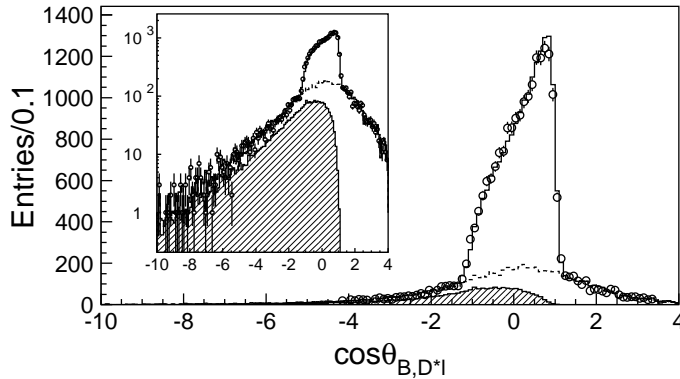


FIG. 1: The $\cos\theta_{B,D^*\ell}$ distribution for the $D^{*-}\ell^+\nu$ candidates. The circles with errors show the data. The solid line is the fit result. The total background and the $D^{**}\ell\nu$ component are shown by the dashed line and the hatched area, respectively. The inset shows the same figure with a logarithmic scale for the vertical axis.

The method of identifying the flavor of the accompanying B meson is described elsewhere [2]. For each flavor decision, we use properties of the remaining tracks in the event to assign a quantity r , which is a MC-determined flavor-tagging dilution factor that ranges from $r = 0$ for no flavor discrimination to $r = 1$ for unambiguous flavor assignment. It is used only to sort data into six intervals of r , according to estimated flavor purity.

To reconstruct the $B^0 \rightarrow D^{*-}\ell^+\nu$ decay vertex, we first form a neutral \overline{D}^0 trajectory. We then reconstruct the B^0 decay vertex using the \overline{D}^0 trajectory, the lepton track and the interaction-point profile (IP) convolved with the finite B flight length in the plane perpendicular to the z axis ($21\ \mu\text{m}$). To ensure good vertex quality, the reduced χ^2 of the vertex is required to be less than 15. The method of reconstructing the tagging side B vertex is described elsewhere [2].

We find 16397 candidates after flavor tagging and vertex reconstruction. The signal fraction is estimated to be 80.4%. The backgrounds consist of fake D^* mesons (7.8%), $B \rightarrow D^{**}\ell\nu$ events (7.4%), random combinations of D^* mesons with leptons with no angular correlation (2.6%; called “uncorrelated background”) and continuum events (1.8%). The background due to a combination of a fake lepton and a true D^* from the same B meson is estimated with MC to be 0.5% and is small enough to be neglected. We estimate the fake D^* background fraction from the \overline{D}^0 mass sideband events and from fake D^*

events reconstructed with wrong-charge slow pions. The uncorrelated background fraction is evaluated by counting candidates where we invert the lepton momentum vector artificially. In this case uncorrelated background in the signal region remains at the same level while the $B^0 \rightarrow D^{*-}\ell^+\nu$ signal events are rejected. We apply the same event selection to off-resonance data (2.3 fb^{-1}) and obtain 24 ± 8 continuum events in the signal region after subtracting the fake D^* background. We estimate the continuum background fraction by scaling this result with the integrated luminosity. We fit the $\cos\theta_{B,D^*\ell}$ distribution in a range $-10 < \cos\theta_{B,D^*\ell} < 1.1$ to estimate the $B \rightarrow D^{**}\ell\nu$ background fraction; the $\cos\theta_{B,D^*\ell}$ shapes for the signal and $B \rightarrow D^{**}\ell\nu$ are modelled using MC and all the other background fractions and distributions are fixed from the aforementioned special background samples.

The Δt resolution function for the signal, $R_{\text{sig}}(\Delta t)$, is expressed as a sum of two Gaussians (a *main* component, plus a *tail* component caused by poorly reconstructed tracks):

$$R_{\text{sig}}(\Delta t) = g_1 G(\Delta t; \mu_1, \sigma_1) + (1 - g_1) G(\Delta t; \mu_2, \sigma_2),$$

$$\sigma_{1(2)} = S_{1(2)} \sqrt{\sigma_{\text{rec}}^2 + \sigma_{\text{tag}}^2},$$

where $G(x; \mu, \sigma)$ is the Gaussian function with μ and σ as the mean and standard deviation, respectively, g_1 is the fraction of the main component, $S_{1(2)}$ is a scale factor that corrects our imperfect error estimation, and $\sigma_{\text{rec(tag)}}$ is the Δt error calculated from the vertex error for the reconstructed (tagged) B meson determined for each event. We extract the above parameters by performing an unbinned maximum-likelihood fit to the Δt distribution of the candidate $B^0 \rightarrow D^{*-}\ell^+\nu$ events without distinguishing between different flavor assignments. The signal probability density function (pdf) is given by

$$F_{\text{sig}}(\Delta t) = \int_{-\infty}^{\infty} \Lambda(\Delta t'; \tau_{B^0}) R_{\text{sig}}(\Delta t - \Delta t') d\Delta t',$$

where $\Lambda(\Delta t; \tau_{B^0}) = \exp(-|\Delta t|/\tau_{B^0})/(2\tau_{B^0})$. We define the likelihood value for each event as $L_i = (1 - f_{\text{bg}})F_{\text{sig}}(\Delta t_i) + f_{\text{bg}}F_{\text{bg}}(\Delta t_i)$, where f_{bg} is the overall background fraction of 0.196 and $F_{\text{bg}}(\Delta t_i)$ is the background pdf given by $\sum_k f_k F_k(\Delta t_i)$. Here F_k and f_k are the pdf and signal fraction, respectively, for each of the four background components. We use the signal pdf for the $B \rightarrow D^{**}\ell\nu$ component. For the other background components, we use $F_k(\Delta t) = \int_{-\infty}^{\infty} [(1 - f_{\delta k})\Lambda(\Delta t'; \tau_k) + f_{\delta k}\delta(\Delta t')] R_k(\Delta t - \Delta t') d\Delta t'$, $R_k(\Delta t) = G(\Delta t; \mu_k, \sigma_k)$, and $\sigma_k = S_k \sqrt{\sigma_{\text{rec}}^2 + \sigma_{\text{tag}}^2}$. To obtain the background parameters in $F_k(\Delta t)$ prior to the $R_{\text{sig}}(\Delta t)$ determination, we fit the Δt distributions for the following background control samples: for fake D^* we use the upper M_{diff} side band, $0.155 < M_{\text{diff}} < 0.165 \text{ GeV}/c^2$; for uncorrelated background we use the lepton-momentum-inverted events; and for continuum background we use off-resonance data, where the selection criteria on the D^* momentum and $\cos\theta_{B,D^*\ell}$ are relaxed to increase the statistics. We perform a likelihood fit to determine $R_{\text{sig}}(\Delta t)$ with fixed background parameters and $\tau_{B^0} = 1.548 \text{ ps}$ [7]. We find that the fraction of the main component is large ($g_1 = 0.87^{+0.06}_{-0.09}$) and the Δt error estimation is correct ($S_1 = 0.99^{+0.09}_{-0.10}$). The typical rms resolution on Δt is 1.43 ps.

We determine Δm_d and wrong tag fractions w_l ($l = 1, 6$) simultaneously by an unbinned maximum-likelihood fit to the Δt distributions. We define the likelihood value for each event as follows:

$$L_i^{\text{OF(SF)}} = (1 - f_{\text{bg}}^l) \{ (1 - f_{D^{**}\ell\nu}^l) F_{\text{sig}}^{\text{OF(SF)}}(\Delta t_i) + f_{D^{**}\ell\nu}^l F_{D^{**}\ell\nu}^{\text{OF(SF)}}(\Delta t_i) \}$$

$$+ f_{\text{bg}}^l \sum_k f_k^l f_{lk}^{\text{OF(SF)}} F_k^{\text{OF(SF)}}(\Delta t_i),$$

where OF (SF) denotes $B^0 \bar{B}^0$ ($B^0 B^0$ or $\bar{B}^0 \bar{B}^0$), i.e. a state with the opposite (same) flavor, $F_{\text{sig}}^{\text{OF(SF)}}$, $F_{D^{**}\ell\nu}^{\text{OF(SF)}}$ and $F_k^{\text{OF(SF)}}$ are pdfs for the OF (SF) signal events, $D^{**}\ell\nu$ decays and other backgrounds, respectively, and f_{bg}^l is an overall background fraction excluding $B \rightarrow D^{**}\ell\nu$ in each r region. Other background fractions $f_{lk}^{\text{OF(SF)}}$, where the relation $f_{lk}^{\text{OF}} + f_{lk}^{\text{SF}} = 1$ holds, are obtained from the control samples for the uncorrelated and fake D^* backgrounds, and from MC events for the continuum.

The pdfs for the OF and SF signal events are given by

$$F_{\text{sig}}^{\text{OF(SF)}}(\Delta t) = \int_{-\infty}^{\infty} \mathcal{P}_{\text{mix}}^{\text{OF(SF)}}(\Delta t') R_{\text{sig}}(\Delta t - \Delta t') d\Delta t',$$

where

$$\mathcal{P}_{\text{mix}}^{\text{OF(SF)}}(\Delta t) = \frac{e^{-|\Delta t|/\tau_{B^0}}}{4\tau_{B^0}} \{1 \pm (1 - 2w_l) \cos(\Delta m_d \Delta t)\}.$$

Since the fake D^* background includes a mixing component, we use a function that is similar to the pdf for $B \rightarrow D^{**}\ell\nu$. The pdf for $B \rightarrow D^{**}\ell\nu$ is given by a sum of B^0 and B^+ components as $F_{D^{**}\ell\nu}^{\text{OF(SF)}}(\Delta t) = (1 - f_{B^+}) F_{\text{sig}}^{\text{OF(SF)}}(\Delta t) + f_{B^+} F_{B^+}^{\text{OF(SF)}}(\Delta t)$, where f_{B^+} is the B^+ fraction in the $B \rightarrow D^{**}\ell\nu$ background. We use the signal pdf for the $B^0 \rightarrow D^{**}\ell^+\nu$ background. The pdfs for the $B^+ \rightarrow D^{**}\ell\nu$ background, $F_{B^+}^{\text{OF(SF)}}(\Delta t)$, are given by the following functions convolved with R_{sig} : $\mathcal{P}_{B^+}^{\text{OF}} = (1 - w_{B^+}^l) \mathcal{P}_{B^+}$ and $\mathcal{P}_{B^+}^{\text{SF}} = w_{B^+}^l \mathcal{P}_{B^+}$, where $\mathcal{P}_{B^+}(\Delta t) = (1 - r_\delta f_\delta) \Lambda(\Delta t; r_{B^+} \tau_{B^+}^l) + r_\delta f_\delta \delta(\Delta t)$ and $w_{B^+}^l$ is the wrong tag fraction for B^+ decays in each r region determined from a $B^+ \rightarrow \bar{D}^0 \pi^+$ control sample.

We perform the fit with 10 free parameters (listed in Table I) to the Δt distributions of SF and OF events in the signal region and the $B \rightarrow D^{**}\ell\nu$ dominant region defined as $-10 < \cos \theta_{B,D^*\ell} < -1.1$. In this way, the background parameters f_{B^+} , f_δ and $\tau_{B^+}^l$ are determined simultaneously. Additional correction factors, r_δ and r_{B^+} , are introduced only in the signal region to account for the difference between the two regions. We use MC to determine $r_\delta = 0.62^{+0.14}_{-0.12}$ and $r_{B^+} = 1.04 \pm 0.02$.

The fit result is summarized in Table I. Figure 2 shows the observed Δt distributions for the OF and SF events. Figure 3 shows the corresponding flavor asymmetry, $\mathcal{A}(\Delta t) = [\text{N}_{\text{OF}}(\Delta t) - \text{N}_{\text{SF}}(\Delta t)] / [\text{N}_{\text{OF}}(\Delta t) + \text{N}_{\text{SF}}(\Delta t)]$, where $\text{N}_{\text{OF(SF)}}$ denotes the number of OF (SF) events.

The sources of systematic error we consider are listed in Table II. One of the largest systematic errors for Δm_d arises from the uncertainties on the D^{**} branching fractions, which have been assumed in the MC but are not known precisely. Each such branching fraction is set in turn to unity in the MC (with all others set to zero), and the analysis is repeated; we take the largest variation on the Δm_d result as the systematic error. To account for uncertainties in the tails of the vertex resolution, we measure Δm_d by setting the upper limit on $|\Delta t|$ that ranges from 5 to 55 ps. We take the largest difference from the main result, which is obtained without the $|\Delta t|$ upper limit, as a systematic error. Systematic errors due to uncertainties in the background pdfs are studied by varying each shape parameter individually and repeating the fit procedure. We add the contribution from each variation in quadrature. We also perform a MC study where we obtain background pdfs by two methods: one from the background control samples, and the other directly from

TABLE I: Summary of mixing fit. Errors are statistical only. For each wrong tag fraction, the r interval and the number of candidate events are also shown.

parameter	result
Δm_d	$0.494 \pm 0.012 \text{ ps}^{-1}$
w_1 ($0 < r \leq 0.25$, 6360 events)	0.467 ± 0.010
w_2 ($0.25 < r \leq 0.5$, 2364 events)	0.360 ± 0.016
w_3 ($0.5 < r \leq 0.625$, 1453 events)	0.254 ± 0.020
w_4 ($0.625 < r \leq 0.75$, 1702 events)	0.182 ± 0.017
w_5 ($0.75 < r \leq 0.875$, 1958 events)	0.103 ± 0.014
w_6 ($0.875 < r \leq 1$, 2560 events)	0.032 ± 0.010
f_{B^+}	$0.70^{+0.12}_{-0.13}$
f_δ	$0.28^{+0.10}_{-0.09}$
τ'_{B^+}	$1.87^{+0.24}_{-0.18} \text{ ps}$

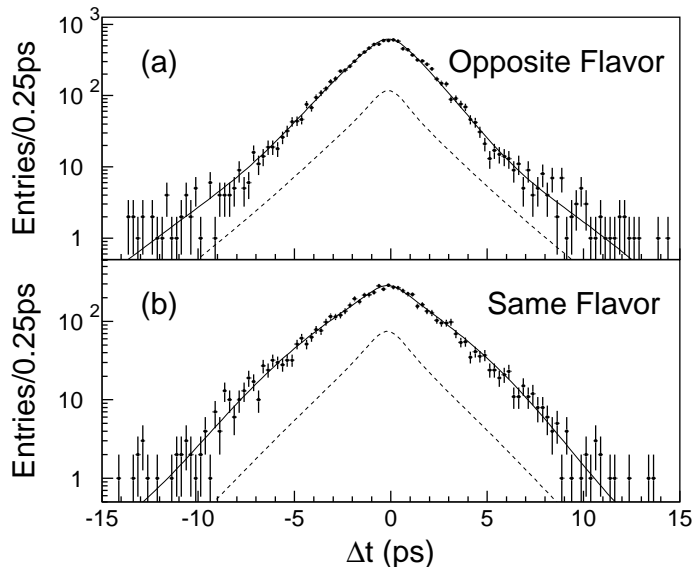


FIG. 2: The Δt distributions for (a) the OF events and (b) the SF events. The solid lines are the result of the unbinned maximum likelihood fit. The dashed lines show the background distribution.

the signal region. The difference between two Δm_d fit results is included in the systematic error due to the uncertainties in the background shape. We generate a large number of $B \rightarrow D^* \ell \nu$ and $B \rightarrow D^{**} \ell \nu$ MC events to test for fit bias. We obtain a Δm_d value that is consistent with the input value to within 1.7σ . We conservatively take the difference, which we attribute to MC statistics, as a systematic uncertainty. The systematic error due to the IP constraint is estimated by varying ($\pm 10\mu\text{m}$) the smearing used to account for the B flight length. Other sources of systematic errors in Table II are obtained by changing each parameter by 1σ , repeating the fit procedure and adding each contribution in quadrature. We also perform a Δm_d fit in each r region. All results are consistent within the statistical

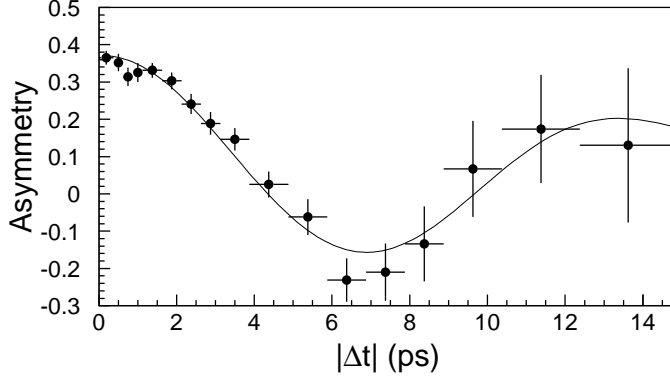


FIG. 3: The observed time-dependent flavor asymmetry. The curve is the result of the unbinned maximum likelihood fit.

TABLE II: Summary of the systematic errors (ps^{-1}) on the Δm_d measurement.

source	error (ps^{-1})
D^{**} branching fractions	0.007
$ \Delta t $ cut	0.007
Background shape	0.006
Resolution function	0.006
B^0 lifetime	0.005
Fit bias	0.004
Background fraction	0.003
$B \rightarrow D^{**}\ell\nu$ fraction	0.002
IP constraint	0.002
B^\pm wrong tag fraction	< 0.001
B^\pm shape parameter	< 0.001
total	0.015

errors and we observe no systematic trend and assign no error.

In summary, we have measured the B^0 - \bar{B}^0 mixing parameter Δm_d using semileptonic $B^0 \rightarrow D^{*-}\ell^+\nu$ decays in a 29.1 fb^{-1} data sample collected with the Belle detector at the KEKB e^+e^- collider operating at the $\Upsilon(4S)$ resonance. From an unbinned maximum likelihood fit to the Δt distributions for B pairs with the same and opposite flavors, we obtain

$$\Delta m_d = 0.494 \pm 0.012(\text{stat}) \pm 0.015(\text{syst}) \text{ ps}^{-1}.$$

The result is one of the most precise measurements performed so far, and is consistent with the world average value of $\Delta m_d = 0.472 \pm 0.017 \text{ (ps}^{-1}\text{)}$ [7] as well as other recent measurements [8].

We wish to thank the KEKB accelerator group for the excellent operation of the KEKB accelerator. We acknowledge support from the Ministry of Education, Culture, Sports, Science, and Technology of Japan and the Japan Society for the Promotion of Science;

the Australian Research Council and the Australian Department of Industry, Science and Resources; the National Science Foundation of China under contract No. 10175071; the Department of Science and Technology of India; the BK21 program of the Ministry of Education of Korea and the CHER SRC program of the Korea Science and Engineering Foundation; the Polish State Committee for Scientific Research under contract No. 2P03B 17017; the Ministry of Science and Technology of the Russian Federation; the Ministry of Education, Science and Sport of the Republic of Slovenia; the National Science Council and the Ministry of Education of Taiwan; and the U.S. Department of Energy.

* on leave from National Fermi Accelerator Laboratory, Batavia IL

† on leave from Nova Gorica Polytechnic, Nova Gorica

- [1] M. Kobayashi and T. Maskawa, Prog. Theor. Phys. **49**, 652 (1973).
- [2] K. Abe *et al.* (Belle Collab.), Phys. Rev. Lett. **87**, 091802 (2001); K. Abe *et al.* (Belle Collab.), hep-ex/0202027, accepted for publication in Phys. Rev. D.
- [3] B. Aubert *et al.* (BaBar Collab.), Phys. Rev. Lett. **87**, 091801 (2001); B. Aubert *et al.* (BaBar Collab.), hep-ex/0201020, submitted to Phys. Rev. D.
- [4] Throughout this Letter, the inclusion of the charge conjugate mode decay is implied.
- [5] E. Kikutani ed., KEK Preprint 2001-157 (2001), to appear in Nucl. Instr. and Meth. A.
- [6] A. Abashian *et al.* (Belle Collab.), Nucl. Instr. and Meth. A **479**, 117 (2002).
- [7] D. E. Groom *et al.* (Particle Data Group), Eur. Phys. J. **C15**, 1 (2000).
- [8] K. Abe *et al.* (Belle Collab.), Phys. Rev. Lett. **86**, 3228 (2000); T. Tomura *et al.* (Belle Collab.), hep-ex/0207022, submitted to Phys. Lett. B; B. Aubert *et al.* (BaBar Collab.), Phys. Rev. Lett. **88**, 221802 (2002); B. Aubert *et al.* (BaBar Collab.), Phys. Rev. Lett. **88**, 221803 (2002).